ACS Medicinal Chemistry Letters

pubs.acs.org/acsmedchemlett

TSPO 18 kDa (PBR) Targeted Photosensitizers for Cancer Imaging (PET) and PDT

Yihui Chen,*[,†,‡] Munawwar Sajjad,*[,‡] Yanfang Wang,[†,§] Carrie Batt,[†] Hani A. Nabi,[‡] and Ravindra K. Pandey*[,†]

[†]PDT Center, Roswell Park Cancer Institute, Buffalo, New York 14263, United States, and [‡]Department of Nuclear Medicine, State University of New York, Buffalo, New York 14214, United States

ABSTRACT Translocator protein (TSPO) 18 kDa overexpression has been observed in a large variety of human cancers, especially breast cancers. PK 11195, an isoquinoline analogue, is one of the ligands of highest TSPO binding affinity. Due to the long biological half life of our photosensitizers, there is a need to label them with a long lived radioisotope, for example I-124. Our objectives are to find translocator protein targeted photosensitizers for both tumor imaging (PET) and photodynamic therapy (PDT). I-PK 11195 is conjugated with the tumor avid photosensitizer HPPH. We find that those two tumor avid components complement each other and make the conjugate molecule even more tumor avid; compared to the photosensitizer itself, the conjugate is found to show improved PDT efficacy. It is concluded that I-PK 11195 can be a good vehicle to deliver radionuclide and photosensitizer to TSPO overexpressed tumor regions. Such conjugates could be useful for both tumor imaging (PET) and PDT.

KEYWORDS Photodynamic therapy (PDT), translocator protein (TSPO), peripheral benzodiazepine receptor (PBR), positron emission tomography (PET), PK 11195, cancer target specific

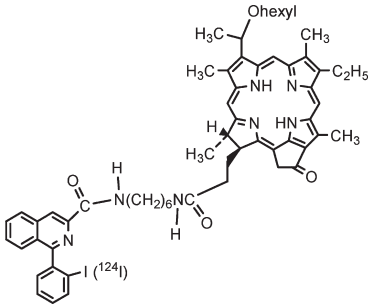

PBR (peripheral benzodiazepine receptor) is suggested to be named Translocator Protein (18 kDa) (TSPO 18 kDa) by Papadopoulos et al.[1] based on its structure and molecular function. TSPO is involved in numerous functions,[2−4] including the role in steroidogenesis and mitochondrial respiration[5,6] and apoptosis regulation.[7−9] A number of findings argue in favor of the development of TSPO targeting approaches in the treatment of human cancers. (i) TSPO overexpression has been observed in a large variety of human cancers,[10] especially in breast cancers.[11] (ii) TSPO is a component of the central regulatory complex of apoptosis;[12] this suggests that TSPO targeting could be of interest in combination with various antitumor therapies. (iii) TSPO binding by high-affinity ligands enhances apoptosis induction of numerous inducers; moreover, TSPO ligands are able to reverse the Bcl-2 cytoprotective effect.[13] For breast cancers, it was reported[11] that TSPO expression and TSPO-mediated cholesterol transport are involved in cell proliferation and aggressive phenotype expression, thus participating in the advancement of the disease. Altogether, these observations justify the use of TSPO ligands in combination with other antitumor therapies for the diagnosis and treatment of breast cancers. Although a number of wide varieties of endogenous and synthetic molecules were reported to have high affinities for TSPO,[14] currently PK 11195 is still the most widely used TSPO ligand and regarded as the gold standard.[15]

Photodynamic therapy (PDT) is a unique approach that uses low energy light to kill cancer cells;[16−20] more selective and potent sensitizers need to be developed. PET (positron emission tomography)[21−23] assesses the functional or metabolic characteristics of the tumor while CT (computed tomography) and MRI (magnetic resonance imaging) mainly assess the tumor's anatomical and morphological features. ^{124}I ($t_{1/2}$ = 4.2 days) is a potential candidate for labeling compounds that have slow clearance kinetics. Pentlow[24] and our group[25] have shown that quantitative imaging with ^{124}I is possible. We were the first who labeled porphyrin by ^{124}I to image cancers,[25] although the PET imaging result of our ^{124}I labeled porphyrin photosensitizer was quite decent, we are still trying to find a more breast cancer specific agent for tumor detection and therapy.

In order to find TSPO targeted bifunctional (PDT and PET) agents, we started from the synthesis of iodo-PK 11195 (**3**). The iodo-PK 11195 (**3**; Scheme 1) was synthesized following the method reported by Gildersleeve et al.[26] Briefly, 2-(2-iodophenyl)-4-benzylidene-5(4H)-oxazolone, which was in turn produced by reacting 2-iodohippuric acid with benzaldehyde, was converted into iodo-PK 11195 carboxylic acid (**2**) under acidic conditions. It was then treated with ethylchloroformate before reacting with *N*-methyl-*sec*-butylamine; the desired isoquinoline analogue (**3**) was obtained in overall 40% yield. In order to convert cold PK 11195 into ^{124}I-PK 11195, we abandoned the isotope exchange approach[26] due to its hard reaction conditions and low yield; instead, we first converted the I-PK 11195 into its stannic derivatives. In an initial experiment, I-PK 11195 (**3**) was

Received Date: September 12, 2010
Accepted Date: November 16, 2010
Published on Web Date: November 23, 2010

© 2010 American Chemical Society

DOI: 10.1021/ml100211g | *ACS Med. Chem. Lett.* **2011**, *2*, 136–141

Scheme 1. Structures and Syntheses of **1**−**22**[a]

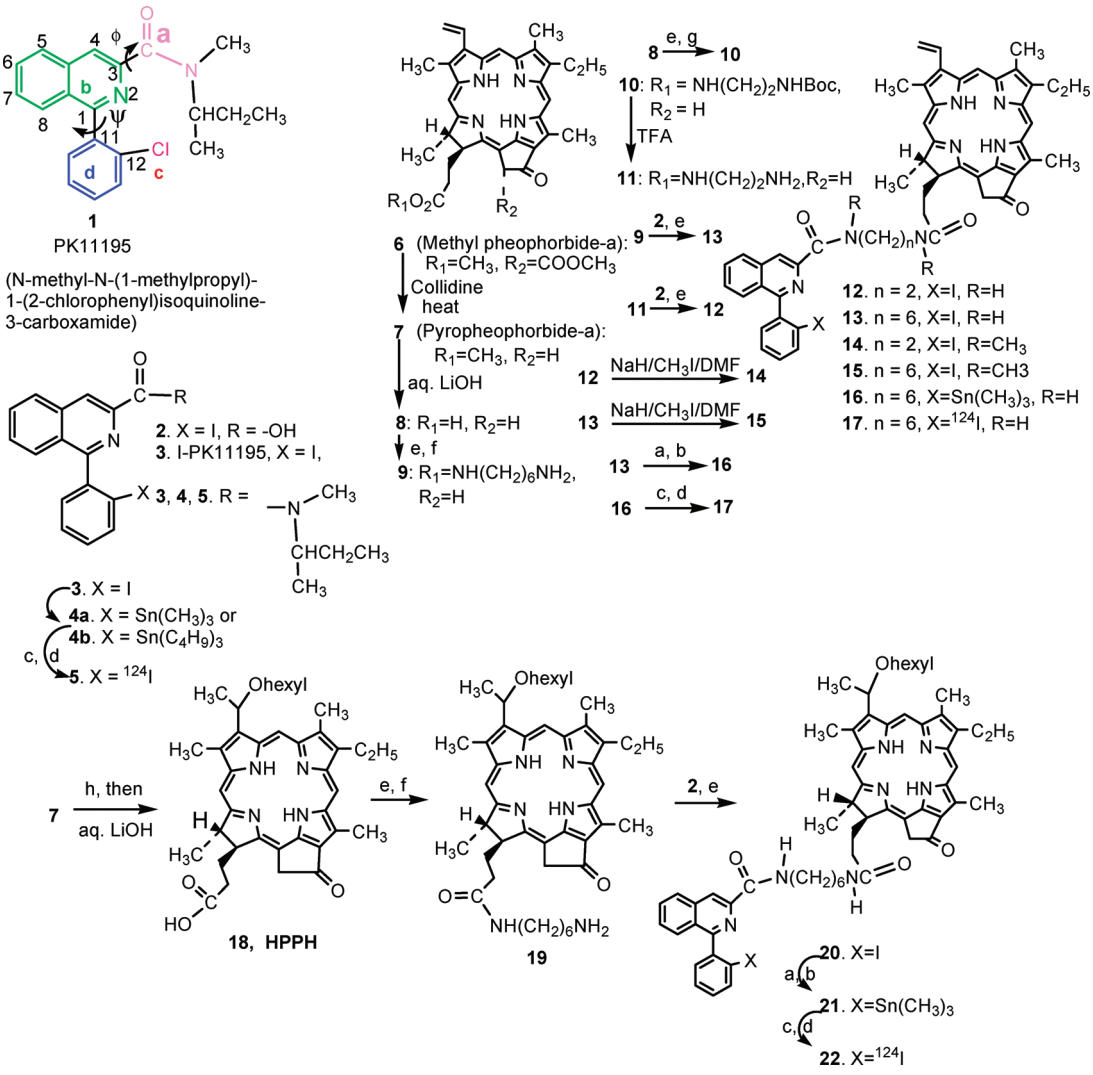

[a] Reagents: (a) $Sn_2(CH_3)_6$ or $Sn_2(C_4H_9)_6$; (b) $PdCl_2(PPh_3)_2$; (c) *N*-chlorosuccinimide; (d) $Na^{124}I$; (e) (benzotriazol-1-yloxy)tris(dimethylamino)phosphonium hexafluorophosphate (BOP); (f) hexamethylene diamine; (g) *N*-Boc-ethylenediamine; (h) HBr in acetic acid and then hexanol.

converted into the trimethylstannyl analogue (**4a**) in 60% yield by reacting **3** with hexamethylditin with the catalysis of *trans*-dichlorobis(triphenylphosphine)palladium(II). Due to the approximately same retention times of **3** and the corresponding trimethylstannyl analogue (**4a**), the separation of these two compounds by HPLC was very difficult. However, replacing the trimethylstannyl group with a tributylstannyl substituent, **4b** (Scheme 1) produced significantly longer HPLC retention time, and we were able to separate both compounds easily by HPLC. **4b** was then converted into ^{124}I-PK 11195 (**5**) by reacting with $Na^{124}I$ in the presence of *N*-chlorosuccinimide, in 60% yield and with >95% radioactive specificity. ^{124}I-PK 11195 (**5**) was purified by HPLC (column: C18, 5 μm, 150 mm × 4.6 mm Adsorborsphere; eluting solvent: 58% MeOH/42% H_2O; flow rate: 1.0 mL/min). The HPLC process was monitored by both UV (328 nm) and radiodetectors. The specific activity of the desired labeled analogue **5** was >1 Ci/μmol.

Methylpheophorbide-a (**6**), obtained from Spirulina Pacifica, was converted into pyropheoporbide-a carboxylic acid (**8**) by following the methodology improved in our laboratory.[25] Upon reaction with BOP [(benzotriazol-1-yloxy)tris(dimethylamino)-phosphonium hexafluorophosphate] and hexamethylene diamine, **8** was converted into amide **9** in 60% yield. By following a similar approach, after reacting with *N*-Boc-ethylenediamine, **8** was converted to **10** in 90% yield. Deprotection of **10** by trifluoroacetic acid produced desired **11** in almost quantitative yield. Compounds **9** and **11** were converted to the conjugate molecules **13** and **12**, respectively, in approximately 70% yield by the reaction with BOP and **2**. **12** and **13** were converted into **14** and **15**, respectively, by reacting with sodium hydride and then methyl iodide in 30% yield. Following the procedure described for the synthesis of **5**, compound **13** was converted into the radiolabeled analogue **17**. Similarly, following the procedure described for the synthesis of **13**, compound **20**, the conjugate

© 2010 American Chemical Society

DOI: 10.1021/ml100211g | *ACS Med. Chem. Lett.* 2011, *2*, 136–141

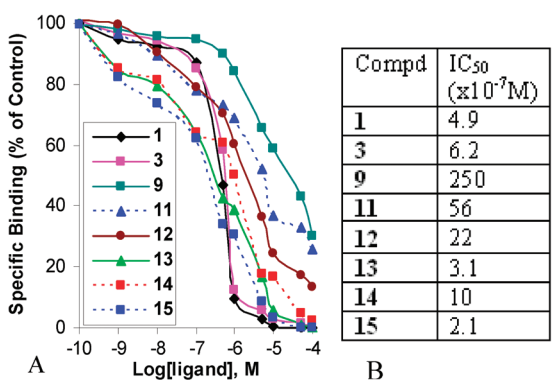

Compd	IC_{50} ($\times 10^{-7}$ M)
1	4.9
3	6.2
9	250
11	56
12	22
13	3.1
14	10
15	2.1

B

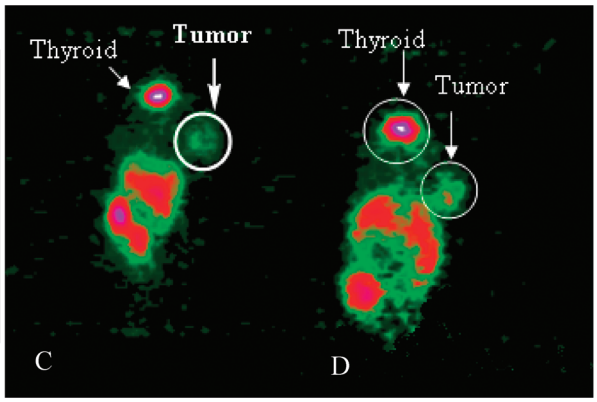

Figure 1. (A) Displacement of ^{3}H-PK 11195 with various compounds; (B) IC_{50} value of various compounds—the concentration of competitor at which 50% of ^{3}H-PK 11195 binding was inhibited; (C and D) microPETemission imaging (coronal view) of Balb/c mice bearing colon-26 (C) and EMT-6 tumors (D) at 24 h p.i. of ^{124}I-**3**; ^{124}I-**3** possesses obvious tumor imaging ability.

of iodo-PK 11195 carboxylic acid (**2**) with **18** (HPPH, 3-[1′-hexyloxyethyl]-3-devinyl pyropheophorbide-a), was also prepared in moderate yield. HPPH is a tumor-avid photosensitizer currently in phase II clinical trials. Following the procedure described for the synthesis of **17**, ^{124}I-labeled **20**, i.e. **22**, was also successfully prepared in a decent yield (Scheme 1). Both **17** and **22** were purified by HPLC (symmetry C18 column; eluting solvent: 95% MeOH/5% H_2O; flow rate: 1.0 mL/min); the specific activity for them was larger than 1 Ci/μmol.

After the preparation of the iodinated PK 11195 **3**, we compared its TSPO binding affinity with that of the parent molecule **1**. As can be seen from Figure 1A and B, replacing the chloro-substituent with an iodo-substituent did not inhibit the TSPO binding affinity. We also investigated the possibility of using ^{124}I-**3** as a tumor imaging agent. As discussed previously, TSPO overexpression has been reported for both colon and breast cancers; therefore, we selected Balb/c mice bearing Colon-26 (colon adenocarcinoma) and EMT6 (well-characterized, undifferentiated mouse breast cancer) tumors. As can be clearly seen from Figure 1 C and D, for both of those tumors, at 24 h postinjection, the tumor sites are clearly defined. Our imaging results were further confirmed by biodistribution study. As can be seen in Figure 2, at early time points, 1 and 2 h postinjection (Figure 2A for Colon-26 tumor) or 4 h postinjection (Figure 2C for EMT6 tumor), tumor uptake of **3** was not conspicuous compared to the cases of other organs; however, at 24 h postinjection, the tumor uptake was just lower than that of liver and stomach (Figure 2B for Colon-26 tumor) or gut (Figure 2D for EMT6 tumor), and it was much higher than that of any other organ. This is obviously due to much a higher drug clearance rate from organs than tumor. To test the ^{124}I-PK 11195 imaging potential for brain cancers, we also investigated the imaging potential of ^{124}I-**3** for nude mouse bearing U87 tumor; U87 cells are glioblastoma cells. Even at 24 h postinjection, we found the tumor uptake was not conspicuous compared to the cases of other organs (Figure 2D). This may be due to the lower TSPO expression in U87 tumor[27] compared to Colon-26 and EMT-6 tumors. Therefore, we concluded that I-PK 11195 is an effective TSPO targeting agent, and it can be used as a vehicle to deliver photosensitizers to the tumor site of specific cancers of high TSPO expression. In the following work, we mainly focused on breast cancer models; breast cancer is one of the deadliest diseases.[28]

The utility of ^{11}C-PK 11195 as PET imaging agent has been reported by Pappata,[29] unfortunately due to a very short half-life of carbon-11 (20 min), it is impractical to use ^{11}C-PK 11195 as the imaging agent for tumors because the drug accumulation needs at least several hours circulation. Tritium labeled PK 11195 is another radiodetectable form of this molecule; however, tritium decays into helium-3 by emission of a low energy β particle, not a positron, so that ^{3}H-PK 11195 cannot be used for PET imaging. In contrast, ^{124}I-PK 11195's longer half-life (4.2 days) enables us to image tumors. Although there are some publications that report using ligands of TSPO to image brain, for example, Chalon et al.[30] reported use of iodinated PK 11195 as an *ex vivo* marker of neuronal injury in the lesioned rat brain, we are the first to use ^{124}I-PK 11195 as the imaging agent for cancers here. In our approach to develop a bifunctional agent for both tumor imaging and phototherapy, we are interested in conjugating I-PK 11195 with photosensitizers. For photosensitizers of low tumor affinity, the idea was to use I-PK 11195 as a vehicle to deliver the photosensitizers to the tumor site; for photosensitizer of high tumor affinity (for example, **18** HPPH), we assume this photosensitizer will facilitate the tumor-targeting of conjugate molecules in some areas of low TSPO expression. Tumors are heterogeneous and mutable and may not have a uniform or consistent expression of a particular receptor, such as TSPO. For the preparation of the desired conjugate, the photosensitizer was linked with PK 11195 by following the reaction sequence illustrated in Scheme 1. In fact, after intensive literature research and analyzing our own experimental results of previous work, we found the structural requirements of PK 11195 analogues for ideal TSPO binding affinity (Scheme 1). In brief they are (a) the long-range electrostatic interactions providing the amide bond in position 3; (b) the bicyclic aromatic system needed to preserve the dihedral angle (Φ); (c) the halogen atom in position 12 that plays some role in the TSPO binding affinity; and (d) the phenyl group needed to preserve the angle (ψ) between the bicyclic system and the phenyl substituent. The TSPO binding affinity data of the conjugates **12**, **13**, **14**, and **15** and intermediates **9** and **11** are summarized in Figure 1A and 1B. It was found that their TSPO binding

© 2010 American Chemical Society

DOI: 10.1021/ml100211g | *ACS Med. Chem. Lett.* **2011**, *2*, 136–141

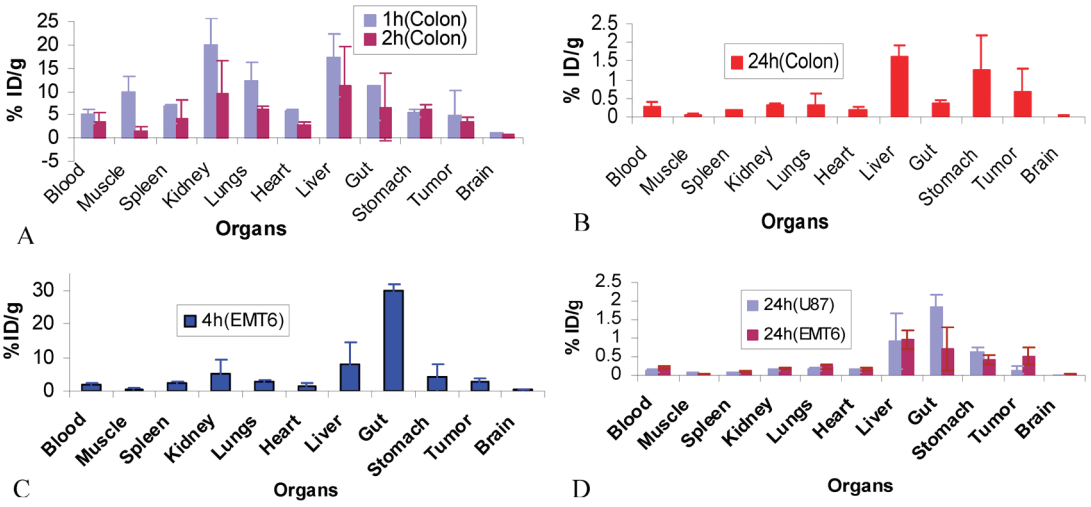

Figure 2. Biodistribution of (^{124}I-labeled) compound **3**. (A and B) Colon-26 tumors (Balb/c mice); (C and D) EMT6 tumors (Balb/c mice) or U87 tumors (nude mice). For Colon-26 tumor, the drug uptakes at 1 h and 2 h postinjection are not conspicuous (A) while the uptake at 24 h postinjection is conspicuous (B); similarly, for EMT6 tumor, the drug uptake at 4 h postinjection is not conspicuous (C) while the uptake at 24 h postinjection is conspicuous (D). For U87 tumor, even at 24 h postinjection, the drug uptake is not conspicuous (D). Standard deviations are presented in error bars.

affinity decreases in this order: **15** ≈ **13** > **14** > **12** > **11** > **9**. It was found that after **9** and **11** were conjugated with **2** (producing **13** and **12**, respectively), their TSPO binding affinities were greatly enhanced; methylation of **12** (producing **14**) enhanced its TSPO binding affinity. In addition, the TSPO binding affinity data of **12** and **13** also indicate that the length of the linkers joining the PK 11195 with the photosensitizer plays a key role in TSPO binding affinity; it is obvious that the six-carbon long linker was more effective than the two-carbon one; maybe this is because that there is no interference to PK 11195's TSPO binding when it is conjugated with photosensitizer by a six-carbon long linker. Considering that the preparation of **15** takes one more step of low yield (30%), and **13** has similar TSPO binding affinity to **15**, we chose the conjugate **13** for further investigations. The dissociation constant (K_d) of **13** binding with TSPO is 40 nM. Conjugate **13** not only showed efficient TSPO binding affinities but also produced a significant tumor avidity determined by ^{124}I-positron emission tomography in both EMT-6 (in Balb-c mice) and MDA-MB-231 (in SCID mice) tumors. We selected MDA-MB-231 (also known as MDA-231) cells, because it was reported[31] that the very aggressive human breast cancer cell line has the highest TSPO expression. Furthermore, it was found that, compared with nonconjugated molecules **9**, **13** produced significantly ($P < 0.001$) higher *in vivo* PDT efficacy in MDA-MB-231 tumors (at 5.0 μmol/kg, 20% tumor-free for **13** versus 0% for **9** at day 60); **8** possesses similar *in vivo* PDT efficacy to **9** (for detailed data, see Supporting Information S-Table 2).

In order to further confirm the target specificity of conjugate molecule **13**, the cellular uptake of **13** and the corresponding nonconjugate **9** were determined by fluorescence spectroscopy. The compounds were excited at 412 nm, and emission was measured over the range 550−750 nm. The maximum emission was at 678 nm. We found that cellular uptake of **13** was more than 2-fold as high as that of **9** (Figure 3A). To further confirm the target specificity of conjugate **13**, I-PK 11195 **3** (at 10 μM, 100 times the concentration of **13** and **9**) was added. It was found that the cellular uptake of **13** was approximately reduced by half, while the uptake of **9** was retained unchanged. This result strongly confirms the TSPO target-specificity of **13**. *In vitro* PDT efficacy itself is a very important indicator for the potential of a photosensitizer; furthermore, investigation of comparative *in vitro* PDT efficacy for the conjugated and nonconjugated photosensitizers is conducive to understanding target specificity. When **13** was added (at a concentration of 0.03 μM) in the presence of **3** (at 2.5 μM, about 85 times the concentration of **13**), inhibition effects were observed at both 24 J/cm^2 and 48 J/cm^2 (Figure 3B). The difficulties for this inhibition experiment are if the concentration of **13** is too low (lower than 0.03 μM), no PDT efficacy can be observed; on the other hand, if the concentration of **3** is too high (higher than 2.5 μM), it will produce toxicity. If just comparing the *in vitro* PDT efficacy, the conjugate molecule **13** produced higher PDT efficacy than the corresponding nonconjugate photosensitizer **9** (Figure 3C). At 1.0 μM, the IC_{50} light doses for **13** and **9** are 0.17 and 0.93 J/cm^2, respectively. Contrarily to the results of EMT-6 and MDA-MB-231 cells, for the TSPO negative Jurkat cells,[27] the cellular drug uptakes of **9** and **13** are similar; no inhibition effect for the *in vitro* efficacy of **13** was observed. In summary, all these results strongly confirm the TSPO target-specificity of **13**.

In order to find photosensitizers of higher PDT efficacy, the conjugate of HPPH **20** was prepared. It was found that **20** possesses similar TSPO binding affinity to **13**. As can be seen from Figure 4A−D, ^{124}I-**20** possesses strong imaging ability. It was also found that **20** did bear stronger tumor affinity than **13**, because the %ID/g value of **20** was higher than that of **13** at every time point; for example, at 24 h postinjection, the %ID/g value for **20** and **13** was 3.87 and 3.28, respectively. The best tumor images for ^{124}I-**20** were obtained at 48, 72, and 96 h postinjection. The long time circulation of compound **20** also further rationalizes the necessity to use I-124 ($t_{1/2}$ 4.2days) rather than F-18 ($t_{1/2}$ 110 min) for the PET imaging. Biodistribution results show that the tumor has

© 2010 American Chemical Society

DOI: 10.1021/ml100211g | *ACS Med. Chem. Lett.* **2011**, *2*, 136–141

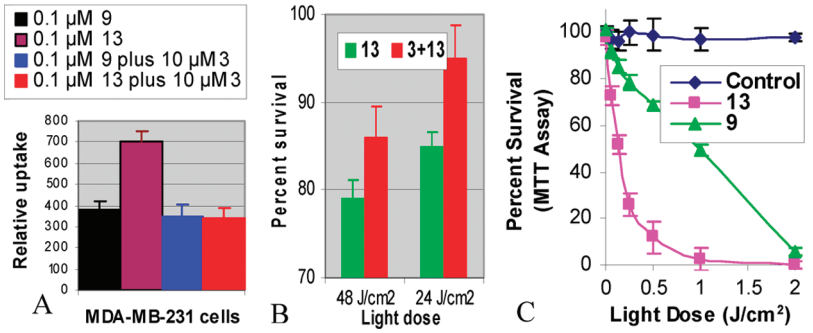

Figure 3. (A) Comparative cellular uptake for **9** and **13** with and without **3**; the presence of **3** decreases the uptake of **13** while it has little effect on the uptake of **9**; (B) *in vitro* PDT efficacy of **13** (0.03 μM) with and without **3** (2.5 μM) on MDA-MB-231 cells; the presence of an ~85 times larger concentration of **3** inhibits the PDT efficacy of **13**; (C) **13** produces better PDT efficacy than **9** (1.0 μM) on MDA-MB-231 cells. Standard deviations are presented in error bars. For EMT6 cells, similar results were obtained.

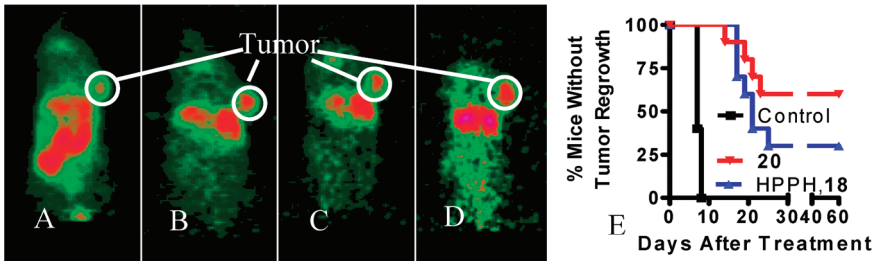

Figure 4. For MDA-231 tumors bearing Scid mice, **22** possesses strong tumor imaging capability. MicroPET emission imaging (coronal view) at 24 h (A), 48 h (B), 72 h (C), and 96 h (D) postinjection of **22** (i.e., ^{124}I-**20**) (dose: 50 μCi (~40 ng)/mouse). (E) Kaplan–Meier plot for the *in vivo* PDT efficacy of compounds HPPH **18** and **20** at 0.4 μmol/kg dose. Light dose: 135 J/cm^2, 75 mW/cm^2, ten mice for each group. **20** produces significantly better *in vivo* PDT efficacy than **18** ($P < 0.0001$).

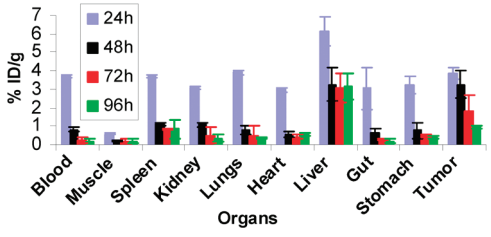

Figure 5. Biodistribution of **22** for MDA-231 tumor bearing Scid mice; tumor has much higher uptake for **22** than any other organs except liver at 48, 72, and 96 h postinjection; three mice for each group. Standard deviations are presented in error bars.

much higher **20** uptake than any other organs except liver at 48, 72, and 96 h postinjection (Figure 5).

Comparative *in vivo* PDT efficacy experiments were also performed in Scid mice bearing MDA-231 tumors (10 mice/group) for **20** and its nonconjugate counterpart **18** HPPH. **20** was found to show much higher efficacy than **18** ($P < 0.0001$) (Figure 4E). Inspiringly, it was also found that, compared to HPPH **18**, **20** produces less skin phototoxicity, which is a major drawback for clinical PDT. The TSPO target-specificity of **20** was also further confirmed by similar experiments described in Figure 3.

In summary, the preliminary results indicate that conjugating the iodo-PK 11195 with PDT agent enhances its target specificity and the PDT efficacy. Currently the study to investigate the synergetic (PDT and chemotherapy) treatment effect for primary and metastatic cancers is in progress.

SUPPORTING INFORMATION AVAILABLE

Synthesis, NMR spectra, elemental analysis of new compounds, experimental procedures of TSPO binding, and *in vitro* and *in vivo* PDT efficacy investigations. This information is available free of charge via the Internet at http://pubs.acs.org.

AUTHOR INFORMATION

Corresponding Author: *Yihui Chen, PDT Center, Cell Stress Biology Department, Roswell Park Cancer Institute, Buffalo, NY 14263. Phone: 716-845-1245. E-mail: yihui.chen@roswellpark.org. Ravindra K. Pandey, PDT Center, Cell Stress Biology Department, Roswell Park Cancer Institute, Buffalo, NY 14263. E-mail: ravindra.pandey@roswellpark.org. Munawwar Sajjad, Department of Nuclear Medicine, State University of New York, Buffalo, NY 14214. E-mail: msajjad@buffalo.edu.

Author Contributions: § Y.W. is on temporary leave from Tongji University, Shanghai, People's Republic of China.

Funding Sources: We thank the National Institutes of Health (1RO1CA127369-O1A1, CA109914) for financial support of this work.

REFERENCES

(1) Papadopoulos, V.; Baraldi, M.; Guilarte, T. R.; Knudsen, T. B.; Lacapere, J.-J.; Lindemann, P.; Norenberg, M. D.; Nutt, D.; Weizman, A.; Zhang, M.-R.; Gavish, M. Translocator protein (18 kDa): new nomenclature for the peripheral-type benzodiazepine receptor based on its structure and molecular function. *Trends Pharmacol. Sci.* **2006,** *27*, 402–409.

© 2010 American Chemical Society

DOI: 10.1021/ml100211g | *ACS Med. Chem. Lett.* **2011**, *2*, 136–141

(2) Kessel, D.; Antolovich, M.; Smith, K. M. The Role of the Peripheral Benzodiazepine Receptor in the Apoptotic Response to Photodynamic Therapy. *Photochem. Photobiol.* **2001,** *74*, 346–349.
(3) Taliani, S.; Settimo, F. D.; Pozzo, E. D.; Chelli, B.; Martini, C. Translocator Protein Ligands as Promising Therapeutic Tools for Anxiety Disorders. *Curr. Med. Chem.* **2009,** *16*, 3359–3380.
(4) Naglar, R.; Savulescu, D.; Krayzler, E.; Leschiner, S.; Veenman, L.; Gavish, M. Cigarette Smoke Decreases Salivary 18 kDa Translocator Protein Binding Affinity—In Association with Oxidative Stress. *Curr. Med. Chem.* **2010,** *17*, 2539–2546.
(5) Gavish, M.; Bachman, I.; Shoukrun, R.; Katz, Y.; Veenman, L.; Weisinger, G.; Weizman, A. Enigma of the peripheral benzodiazepine receptor. *Pharmacol. Rev.* **1999,** *51*, 629–650.
(6) Veenman, L.; Gavish, M. The peripheral-type benzodiazepine receptor and the cardiovascular system: implications for drug development. *Pharmacol. Ther.* **2006,** *110*, 503–524.
(7) Veenman, L.; Papadopoulos, V.; Gavish, M. Channel-like functions of the 18-kDa translocator protein (TSPO): regulation of apoptosis and steroidogenesis as part of the host-defense response. *Curr. Pharm. Des.* **2007,** *13*, 2385–2405.
(8) Kugler, W.; Veenman, L.; Shandalov, Y.; Leschiner, S.; Spanier, I.; Lakomek, M.; Gavish, M. Ligands of the mitochondrial 18 kDa Translocator Protein attenuate apoptosis in human glioblastoma cells exposed to erucylphosphohomocholine. *Cell. Oncol.* **2008,** *30*, 435–450.
(9) Shoukrun, R.; Veenman, L.; Shandalov, Y.; Leschiner, S.; Spanier, I.; Karry, R.; Katz, Y.; Weisinger, G.; Weizman, A.; Gavish, M. The 18 kDa Translocator Protein, formerly known as the peripheral-type benzodiazepine receptor, confers pro-apoptotic and anti-neoplastic effects in a human colorectal cancer cell line. *Pharmacogenet. Genomics* **2008,** *18*, 977–988.
(10) Maaser, K.; Hopfner, M.; Jansen, A.; Weisinger, G.; Gavish, M.; Kozikowski, A. P. Specific ligands of the peripheral benzodiazepine receptor induce apoptosis and cell cycle arrest in human colorectal cancer cells. *Br. J. Cancer* **2001,** *85*, 1771–1780.
(11) Sanger, N.; Strohmeier, R.; Kaufmann, M.; Kuhl, H. Cell cycle-related expression and ligand binding of peripheral benzodiazepine receptor in human breast cancer cell lines. *Eur. J. Cancer* **2000,** *36*, 2157–2163.
(12) Sutter, A. P.; Maaser, K.; Höpfner, M.; Barthel, B.; Grabowski, P.; Faiss, S.; Carayon, P.; Zeitz, M.; Hans Scherübl, H. Specific ligands of the peripheral benzodiazepine receptor induce apoptosis and cell cycle arrest in human esophageal cancer cells. *Radiat. Oncol. Invest.* **2002,** *4*, 318–327.
(13) Hirsch, T.; Decaudin, D.; Susin, S. A.; Marchetti, P.; Larochette, N.; Resche-Rigon, M.; Kroemer, G. PK11195, a ligand of the mitochondrial benzodiazepine receptor, facilitates the induction of apoptosis and reverses Bcl-2-mediated cytoprotection. *Exp. Cell Res.* **1998,** *241*, 426–434.
(14) James, M. L.; Selleri, S.; Kassiou, M. Development of ligands for peripheral benzodiazepine receptor. *Curr. Med. Chem.* **2006,** *13*, 1991–2001.
(15) Han, Z.; Slack, R. S.; Li, W. P.; Papadopoulos, V. Expression of Peripheral Benzodiazepine Receptor (PBR) in Human Tumors: Relationship to Breast, Colorectal, and Prostate Tumor Progression. *J. Recept. Signal Transduct. Res.* **2003,** *23*, 225–238.
(16) Huang, Z. A review of progress in clinical photodynamic therapy. *Technol. Cancer Res. Treat.* **2005,** *4*, 283–293.
(17) Mang, T. S.; Allison, R.; Hewson, G.; Snider, W.; Moskowitz, R. A phase II/III clinical study of tin ethyl etiopurpurin (Purlytin)-induced photodynamic therapy for the treatment of recurrent cutaneous metastatic breast cancer. *Cancer J.* **1998,** *6*, 378–384.
(18) Cuenca, R. E.; Allison, R. R.; Sibata, C.; Downie, G. H. Breast cancer with chest wall progression: Treatment with photodynamic therapy. *Ann. Surg. Oncol.* **2004,** *11*, 322–327.
(19) Wyss, P.; Schwarz, V.; Dobler-Girdziunaite, D.; Hornung, R.; Walt, H.; Degen, A; Fehr, M. K. Photodynamic therapy of locoregional breast cancer recurrences using a chlorin-type photosensitizer. *Int. J. Cancer* **2001,** *93*, 720–724.
(20) Allison, R.; Mang, T.; Hewson, G.; Snider, W.; Dougherty, D. Photodynamic therapy for chest wall progression from breast carcinoma is an underutilized treatment modality. *Cancer* **2001,** *91* (1), 1–8.
(21) Quon, A.; Gambhir, S. S. FDG-PET and beyond: Molecular breast cancer imaging. *J. Clin. Oncol.* **2005,** *23*, 1664–1673.
(22) Fischer, B. M.; Olsen, M. W. B.; Ley, C. D.; Klausen, T. L.; Mortensen, J.; Hojgaard, L.; Kristjansen, P. E. G. How few cancer cells can be detected by positron emission tomography? A frequent question addressed by an in vitro study. *Eur. J. Nucl. Med. Mol. Imaging* **2006,** *33*, 697–702.
(23) Kennedy, J. A.; Israel, O.; Frenkel, A.; Bar-Shalom, R.; Azhari, H. Super-Resolution in PET Imaging. *IEEE Trans. Med. Imaging* **2006,** *25*, 137–147.
(24) Pentlow, K. S.; Graham, M. C.; Lambrecht, R. M.; Daghighian, F.; Bacharach, S. L.; Bendriem, B.; Finn, R. D.; Jordon, K.; Kalaigian, H.; Karp, J. S.; Robeson, W. R.; Larson, S. M. Quantitive Imaging of Iodine-124 with PET. *J. Nucl. Med.* **1996,** *37*, 1557–1562.
(25) Pandey, S. K.; Gryshuk, A.; Sajjad, M.; Zheng, X.; Chen, Y.; Abouzeid, M. M.; Morgan, J.; Charamisinau, I.; Nabi, H. A.; Oseroff, A.; Pandey, R. K. Multimodality Agents for Tumor Imaging (PET, Fluorescence) and Photodynamic Therapy. A Possible "See and Treat" Approach. *J. Med. Chem.* **2005,** *48*, 6286–6295.
(26) Gildersleeve, D. L.; Van Dort, M. E.; Johnson, J. W.; Sherman, P. S.; Wieland, D. M. Synthesis and evaluation of [^{123}I]-Iodo-PK11195 for mapping peripheral-type benzodiazepine receptors (ω3) in heart. *Nucl. Med. Biol.* **1996,** *23*, 23–28.
(27) Mukhopadhyay, S.; Mukherjee, S.; Das, S. K. Increased expression of peripheral benzodiazepine receptor (PBR) in dimethylbenz[*a*]anthracene-induced mammary tumors in rats. *Glycoconj. J.* **2006,** *23*, 199–207.
(28) NCI website: http://ha.cancer.gov/cancertopics/types/breast.
(29) Pappata, S.; Cornu, S.; Samson, Y.; Prenant, C.; Benavides, J.; Scatton, B.; Crouzel, C.; Hauw, J. J.; Syrota, A. PET study of carbon-11-PK 11195 binding to peripheral type benzodiazepine sites in glioblastoma: a case report. *J. Nucl. Med.* **1991,** *32*, 1608–1610.
(30) Chalon, S.; Pellevoisin, C.; Bodard, S.; Vilar, M.-P.; Besnard, J.-C.; Guilloteau, D. Iodinated PK 11195 as an *ex vivo* marker of neuronal injury in the lesioned rat brain. *Synapse* **1996,** *24*, 334–339.
(31) Hardwick, M.; Fertikh, D.; Culty, M.; Li, H.; Vidic, B.; Papadopoulos, V. Peripheral-type benzodiazepine receptor (PBR) in human breast cancer: correlation of breast cancer cell aggressive phenotype with PBR expression, nuclear localization, and PBR-mediated cell proliferation and nuclear transport of cholesterol. *Cancer Res.* **1999,** *59*, 831–842.

© 2010 American Chemical Society

DOI: 10.1021/ml100211g | *ACS Med. Chem. Lett.* **2011,** *2*, 136–141